

Multiscale analysis of heart rate, blood pressure and respiration time series

L. Angelini^{1,2,3}, R. Maestri⁴, D. Marinazzo^{1,2,3}, L. Nitti^{1,3,5}, M.

Pellicoro^{1,2,3}, G. D. Pinna⁴, S. Stramaglia^{1,2,3}, S.A. Tuppiti²

¹*TIRES-Center of Innovative Technologies for Signal Detection and Processing,
Università di Bari, Italy*

²*Dipartimento Interateneo di Fisica, Italy*

³*Istituto Nazionale di Fisica Nucleare,
Sezione di Bari, Italy*

⁴*Dipartimento di Bioingegneria,
Fondazione S. Maugeri, IRCCS,
Istituto Scientifico di Montescano (PV), Italy*

⁵*Dipartimento di Biochimica Medica,
Biologia Medica e Fisica Medica,
University of Bari, Italy*

(Dated: July 24, 2018)

We present the multiscale entropy analysis of short term physiological time series of simultaneously acquired samples of heart rate, blood pressure and lung volume, from healthy subjects and from subjects with Chronic Heart Failure. Evaluating the complexity of signals at the multiple time scales inherent in physiologic dynamics, we find that healthy subjects show more complex time series at large time scales; on the other hand, at fast time scales, which are more influenced by respiration, the pathologic dynamics of blood pressure is the most random. These results robustly separate healthy and pathologic groups. We also propose a multiscale approach to evaluate interactions between time series, by performing a multivariate autoregressive modelling of the coarse grained time series: this analysis provides several new quantitative indicators which are statistically correlated with the pathology.

PACS numbers: 05.10.-a, 87.10.+e, 89.19.Hh

I. INTRODUCTION

Physiological systems are ruled by mechanisms operating across multiple temporal scales. Many approaches have been developed in the last years to analyze these complex signals, including, for example, studies of: Fourier spectra [1], chaotic dynamics [2], scaling properties [3], multifractal properties [4], correlation integrals [5], $1/f$ spectra [6] and synchronization properties [7]. A recently proposed approach, multiscale entropy analysis (MSE) [8], compares the degree of complexity of time series at varying temporal scale, and has been applied to 24 hours electrocardiographic recordings of healthy subjects, subjects with congestive heart failure, and subjects with atrial fibrillation. Results from this analysis support the general *complexity – loss* theory of aging and disease, since healthy and young dynamics are the most complex.

In this paper we apply the MSE analysis to short-term simultaneous recordings of electrocardiogram, respiration signal and arterial blood pressure, from healthy subjects and from subjects with Chronic Heart Failure (CHF), a disease associated with major abnormalities of autonomic cardiovascular control.

We also consider here a multiscale version of the classical multivariate autoregressive analysis of time series, to find scale-dependent patterns of interactions between the physiological time series here considered. The paper is organized as follows. In the next section we describe our data set, the methods and the results we obtain. Some conclusions are drawn in section III.

II. DATA, METHODS AND RESULTS

We briefly recall the MSE method [8]. Given a one-dimensional discrete time series, consecutive coarse grained time series, corresponding to scale factor τ , are constructed in the following way. First, the original time series is divided into nonoverlapping windows of length τ ; then, data points inside each window are averaged, so as to remove fluctuations with time scales smaller than τ . For scale one, the coarse grained time series is simply the original time series; the length of each coarse grained time series is equal to the length of the original time series divided by the scale factor τ . Finally an entropy measure S_E is calculated for each coarse grained time series and plotted as function of the scale factor τ . S_E coincides with the parameter $S_E(m, r)$, introduced by Richman and Moorman [9] and termed *sample entropy*, which is related to the probability that sequences from the time series, which are close (within r)

for m points, remain close at the subsequent data point. In the original proposal both the sequence length m and the tolerance parameter r were kept fixed as τ was varied, so that changes in S_E on each scale were depending both on the regularity and the variability of the coarse grained sequences [10]. In the present work we take r , at each τ , inversely proportional to the standard deviation (SD) of the coarse grained time series, and consider separately how the SD of signals varies with the time scale.

Our data are from 47 healthy subjects and 275 stable mild to moderate CHF patients in sinus rhythm admitted to the Heart Failure Unit of the Scientific Institute of Montescano for evaluation and treatment of heart failure, usually in conjunction with evaluation for heart transplantation. Concerning the second group, cardiac death occurred in 54 patients during a 3-year-follow-up. In two different conditions of respiration, basal and paced breathing (at 0.25 Hz) [11], ten minutes long physiological recordings have been made on these subjects, leading to four time series. Firstly, the heart RR interval time series (rr_i); for each cardiac cycle, corresponding values of the systolic arterial pressure sap , the diastolic arterial pressure dap and the instantaneous lung volume ilv were computed. The four time series have then been re-sampled at 2Hz using a cubic spline interpolation. Part of this data set (the sap time series) has been already analyzed in [12] using a different approach.

In figure 1 we depict the standard deviations of the coarse grained time series in basal condition. Due to the short length of the samples at our disposal, we consider $\tau \leq 10$ so as to have sufficient statistics at each scale; this implies that our analysis will be limited to part of the High Frequency (HF) band (0.15-0.45Hz), the band in which the respiratory rhythm of most people lies. In all cases, on average the standard deviation is a decreasing function of the scale; healthy subjects show greater variability than patients, except for ilv signals, where patients on average have the highest variability. Similar patterns of standard deviations are obtained in paced breathing conditions.

As already stated, to extract the sample entropy from these signals, we take r equal to a fixed percentage (15%) of the standard deviations of the coarse grained time series; we take $m = 1$. In figure 2 we depict the average S_E of rr_i time series of controls, patients and dead patients, in basal condition (high) and paced breathing (low). Concerning the basal case, we note that controls have always significantly higher entropy than CHF patients, at all scales, and that dead patients show slightly more regular rr_i time series than the average over all patients. The severity of the pathology seems to be correlated with the loss of entropy. On the right we depict, as a function of the scale factor τ , the probability that rr_i entropy values from controls and patients were drawn from the same distribution, evaluated by non parametric rank sum Wilcoxon test: the discrimination is excellent at intermediate τ 's. This picture is in agreement with findings in [8], corresponding to controls and subjects with congestive heart failure in sinus rhythm, except for a different form of the entropy curve for patients, which indeed depends on the pathology. In the case of paced breathing the three curves get closer and the discrimination, between patients and controls, reduces: paced breathing seems, in the case of rr_i entropy, to reduce differences between patients and controls.

In figure 3 we depict S_E of sap time series. We find that at low τ patients have higher entropy, whilst at large τ they have lower entropy than controls. The crossover occurs at $\tau = 3$ in basal conditions, and $\tau \sim 6$ for paced breathing. The *complexity - loss* paradigm, hence, here holds only for large τ . This may be explained as an effect of respiration, whose influence seems to become weaker as τ increases. This effect is more evident in conditions of paced breathing. Our results are consistent with those obtained in [12] using a different approach and with $\tau = 1$. It is interesting to observe that curves corresponding to dead patients are always farther, from the controls curve, than the average curve from all patients; departure from the controls curve seems to be connected with the severity of the disease.

In figure 4 we consider dap time series. We find a similar pattern to sap : patients have higher entropy at low τ and lower entropy than controls at large τ . Again the crossover occurs at $\tau = 3$ in basal conditions, and $\tau = 6$ for paced breathing.

Now we turn to consider ilv time series, as depicted in figure 5. In the basal case, controls have higher entropy at small scales. On the other hand controls show lower entropy than patients at $\tau > 7$: patients pathologically display fluctuations of ilv at larger scales than healthy subjects. Under paced breathing, controls are characterized by reduced fluctuations at high τ ; at $\tau = 4$, when the window size is half of the respiration period, controls show a local minimum of the entropy. These phenomena are not observed for patients, where paced breathing is less effective in regularizing the ilv time series.

Next we implement a multiscale version of autoregressive modelling of time series (see, e.g., [13]). For each scale factor τ , we denote $\mathbf{x} = (rr_i, sap, dap, ilv)$ the four-dimensional vector of the coarse grained time series. At each scale, all coarse grained time series are normalized to have unit variance. A multivariate autoregressive model of unity order is then fitted (by standard least squares minimization) to data:

$$\mathbf{x}(t) = A \mathbf{x}(t - 1); \quad (1)$$

A is a 4×4 matrix, depending on τ , whose element A_{ij} measure the causal influence of $j - th$ time series on the $i - th$ one. Some of these matrix elements are found to be significantly different in patients and controls, as described in the following.

Firstly we consider the interactions between heart rate and blood pressure. In physiological conditions heart rate and arterial pressure are likely to affect each other as a consequence of the simultaneous feedback baroreflex regulation from *sap-dap* to *rri* and feedforward mechanical influence from *rri* to *sap-dap* [14].

In figure 6 the curves representing the causal relationship $rri \rightarrow sap$ are represented. Both in basal and paced breathing conditions, this coefficient is always negative and is stronger for controls. Two mechanisms determine the feedforward influence $rri \rightarrow sap$. Firstly the Starling law, stating that when the diastolic filling of the heart is increased or decreased with a given volume, the volume of blood which is then ejected from the heart increases or decreases by the same amount. More blood in: more blood out. This mechanism favors an increase of *sap-dap* as the *rri* interval increases, i.e. a positive coefficient $rri \rightarrow sap$. The second mechanism is diastolic decay, described by the Windkessel model of the capacitative property of arteries; as *rri* interval increases, this effect tends to lower *sap-dap* values and gives a negative contribution to the coefficient $rri \rightarrow sap$. Our finding suggests that the second mechanism is dominant. The difference between patients and controls is significant at low and intermediate τ , and especially in basal conditions. The coefficient $rri \rightarrow dap$ shows a behavior very similar to those of $rri \rightarrow sap$, i.e. it is always negative and is stronger for controls.

Evaluation of baroreflex regulation $sap-dap \rightarrow rri$ is an important clinical tool for diagnosis and prognosis in a variety of cardiac diseases [15]. Recent studies, see e.g. [16] and references therein, have suggested that spontaneous fluctuations of arterial pressure and *rri* offer a noninvasive method for assessing baroreflex sensitivity without use of provocative tests employing injection of a vasoconstrictive drug or manipulation of carotid baroreceptor. In fig. 7 we depict the interaction $dap \rightarrow rri$ as extracted by our approach, showing high discrimination between controls and patients. In basal conditions this coefficient is positive for controls and negative for patients. Moreover, this coefficient for patients is much influenced by respiration: in paced breathing conditions it is almost zero for patients, while being positive for controls. It is worth stressing that the interaction $dap \rightarrow rri$, evaluated by the present approach, has only little relation with the baroreflex sensitivity index considered, e.g., in [16]; indeed the procedures for evaluating these quantities differ in several steps. For example in our approach all time series are centered and normalized, hence the interaction between arterial pressure and *rri* is described only qualitatively.

Human respiration interacts with heart rate, originating the well known phenomenon of respiratory sinus arrhythmia [17]. We find that the interaction $rri \rightarrow ilv$ is significantly ($p < 10^{-4}$) stronger in controls than patients, under paced breathing and using $\tau = 4$. We also find that the interaction $ilv \rightarrow rri$ is positive and significantly ($p < 10^{-5}$) stronger in controls, in basal conditions and at high frequencies ($\tau \leq 4$).

Let us now turn to consider *self interactions* of time series. The matrix element A_{11} describes how much the *rri* signal depends on its value at the previous time. As it is shown in figure 8, in basal conditions A_{11} is significantly lower for controls. In paced breathing conditions significant difference is found at high τ . Also the self interaction of *dap* time series gives rise to an interesting pattern. It is stronger for controls, especially at low τ , leading to high discrimination between controls and patients at low τ as figure 9 shows.

The interaction of systolic and diastolic arterial pressure in healthy subjects has been recently studied in [18]. In the present analysis we find significant differences between patients and controls when the interaction $sap \rightarrow dap$ is considered, see figure 10. For controls, this coefficient is always negative and its strength increases with τ .

It is known that respiration interacts in an open loop way with arterial pressure, mainly through a mechanical mechanism [19]. Our findings confirm it; indeed we find no significant $sap \rightarrow ilv$ interaction, but significant ($p < 10^{-3}$) differences between patients and controls are found when the interaction $ilv \rightarrow sap$ is considered: controls show reduced interaction w.r.t. patients.

III. CONCLUSIONS

In the present paper we have presented the multiscale entropy analysis of short term physiological time series. We have shown that the analysis of [8] can be successfully performed also on short *rri* recordings, still leading to separation between controls and patients. Moreover we extend the analysis by considering simultaneously acquired recordings of *sap*, *dap* and *ilv*. We have also proposed a multiscale approach to evaluate interactions between time series, by performing a multivariate autoregressive modelling of the coarse grained time series. This analysis has put in evidence interesting patterns of interactions between time series, while providing several new quantitative indicators which are statistically correlated with the CHF pathology, and which can be employed for diagnosis of CHF patients. Separating dead patients from alive patients is a very important task, since a good estimation of the probability of surviving of a given patient would be valuable when a decision has to be made with respect to the therapy to be undertaken. The separating performances provided by our indicators in this case are not good as those obtained separating patients and controls. Further work must be done to deal with the separation between dead patients and alive patients; in particular it will be interesting to repeat this analysis with longer recordings so as to take into account fluctuations

in lower frequency bands.

-
- [1] S. Akselrod, D. Gordon, F.A. Ubel, D.C. Shannon and R.J. Cohen, *Science* **213** 220(1981); G.D. Pinna, R. Maestri, G. Raczak, and M.T. La Rovere, *Clin Sci (Lond)* **103** 81 (2002).
- [2] G.A. Babloyantz, J.M. Salazar and C. Nicolis, *Phys. Lett. A* **111** 152(1985); C.S. Poon, C.K. Merrill, *Nature* **389** 492 (1997).
- [3] L.A. Nunes Amaral, A.L. Goldberger, P.C. Ivanov and H.E. Stanley, *Phys. Rev. Lett.* **81** 2388(1998); Y. Ashkenazy, P.C. Ivanov, S. Havlin, C.K. Peng, A.L. Goldberger and H.E. Stanley, *Phys. Rev. Lett.* **86** 1900 (2001).
- [4] P.C. Ivanov, L.A. Nunes Amaral, A.L. Goldberger, S. Havlin, M.G. Rosenblum, Z. Struzik, and H.E. Stanley, *Nature* **399** 461 (1999); L.A. Nunes Amaral, P.C. Ivanov, N. Aoyagi, I. Hidaka, S. Tomono, A.L. Goldberger, H.E. Stanley and Y. Yamamoto, *Phys. Rev. Lett.* **86** 6026 (2001).
- [5] K. Lehnertz, C.E. Elger, *Phys. Rev. Lett.* **80** 5019 (1998).
- [6] C.K. Peng, J. Mietus, J.M. Hausdorff, S. Havlin, H.E. Stanley and A.L. Goldberger *Phys. Rev. Lett.* **70** 1343 (1993); P.C. Ivanov, L.A. Nunes Amaral, A.L. Goldberger, S. Havlin, M.G. Rosenblum, Z. Struzik and H.E. Stanley, *Chaos* **11** 641 (2001).
- [7] P. Tass, M.G. Rosenblum, J. Weule, J. Kurths, A. Pikovsky, J. Volkman, A. Schnitzler, H-J Freund H-J, *Phys. Rev. Lett.* **81** 3291 (1998).
- [8] M. Costa, A.L. Goldberger, C.K. Peng, *Phys. Rev. Lett.* **89** 68102 (2002); M. Costa, A.L. Goldberger, C.K. Peng, *Phys. Rev. E* **71** 21906 (2005).
- [9] J.S. Richman and J.R. Moorman, *Am. J. Physiol.* **278** H2039 (2000); A.L. Goldberger, C.K. Peng, L.A. Lipsitz, *Neurobiol. Aging* **23** 23 (2002).
- [10] Vadim V. Nikulin and Tom Brismar *Phys. Rev. Lett.* **92**, 089803 (2004) ; M. Costa, A.L. Goldberger, C.K. Peng, *Phys. Rev. Lett.* **92**, 089804 (2004).
- [11] S. Rzecziński, N.B. Janson, A.G. Balanov and P.V.E. McClintock, *Phys. Rev. E* **66** 051909 (2002).
- [12] N. Ancona, R. Maestri, D. Marinazzo, L. Nitti, M. Pellicoro, G.D. Pinna, S. Stramaglia, *Physiol. Meas.* **26** 363 (2005).
- [13] H. Kantz and T. Schreiber, *Nonlinear time series analysis* Cambridge University Press, 1997.
- [14] *Mechanisms of blood pressure waves*, K. Miyakawa, C. Polosa, H.P. Koepchen (eds.). Springer, Berlin Heidelberg New York (1984).
- [15] G.D. Pinna, R. Maestri, S. Capomolla, O. Febo, E. Robbi, F. Cobelli, M.T. La Rovere, *J Am Coll Cardiol* **46** 1314 (2005).
- [16] G. Nollo, L. Faes, A. Porta, R. Antolini, F. Ravelli, *Am. J. Physiol. Heart Circ. Physiol.* **288** H1777 (2005).
- [17] J.A. Hirsch, B. Bishop, *Am. J. Physiol.* **241**, H620 (1981); C. Schafer, M.G. Rosenblum, H. Abel, *Nature* **392** 239 (1998); C. Schafer, M.G. Rosenblum, H. Abel, J. Kurths, *Phys. Rev. E* **60** 857 (1999).
- [18] L. Angelini, G. Lattanzi, R. Maestri, D. Marinazzo, G. Nardulli, L. Nitti, M. Pellicoro, G.D. Pinna, and S. Stramaglia, *Phys. Rev. E* **69**, 061923 (2004).
- [19] R.W. de Boer, J.M. Karemaker, J. Strackee, *Am. J. Physiol.* **253**, H680 (1987).
- [20] J.A. Swets, *Science* **240** 1285 (1988).

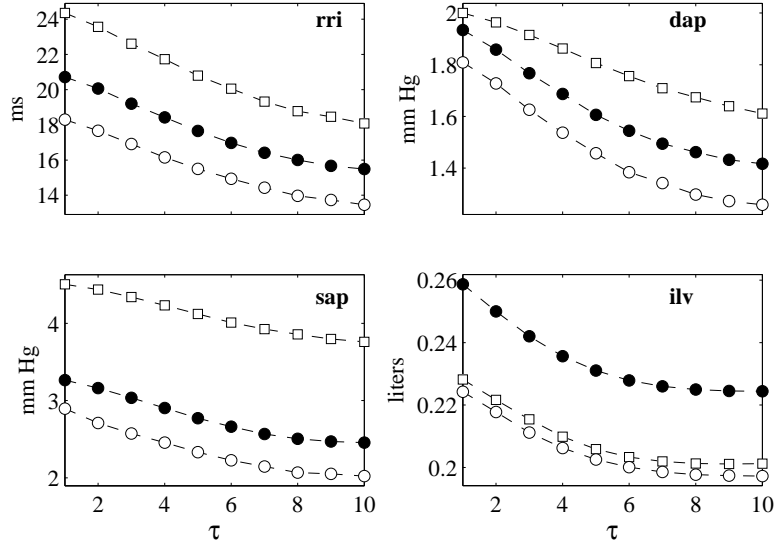


FIG. 1: Standard deviations are plotted versus τ for the coarse grained time series, in basal condition. Empty squares are the averages over the 47 healthy subjects, full circles are the averages over the 275 CHF patients, and empty circles are the averages over the 54 patients for whom cardiac death occurred. Top left: SD of *rri* time series. Top right: SD of *dap* time series. Bottom left: SD of *sap* time series. Bottom right: SD of *ilv* time series.

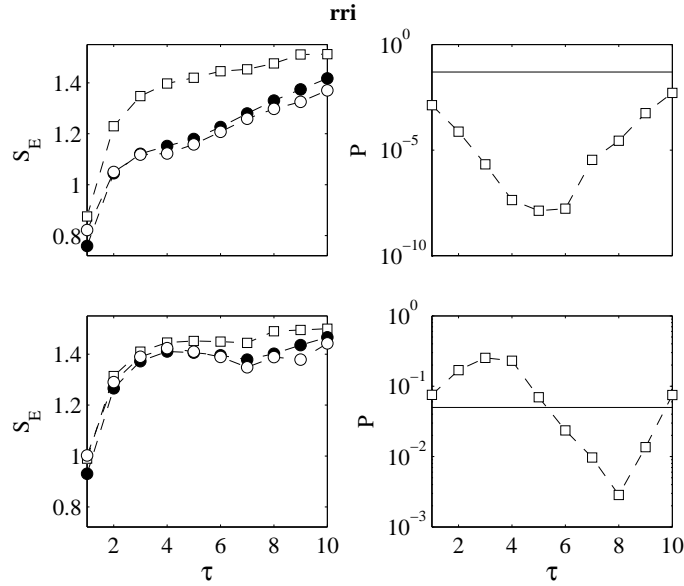


FIG. 2: Sample entropy of *rri* time series plotted versus τ . Empty squares are the averages over the 47 healthy subjects, full circles are the averages over the 275 CHF patients, and empty circles are the averages over the 54 patients for whom cardiac death occurred. Top left: S_E in basal condition. Top right: the probability that basal S_E values from controls and patients were drawn from the same distribution, evaluated by non parametric test. Bottom left: S_E in paced breathing condition. Bottom right: the probability that paced breathing S_E values from controls and patients were drawn from the same distribution, evaluated by non parametric test.

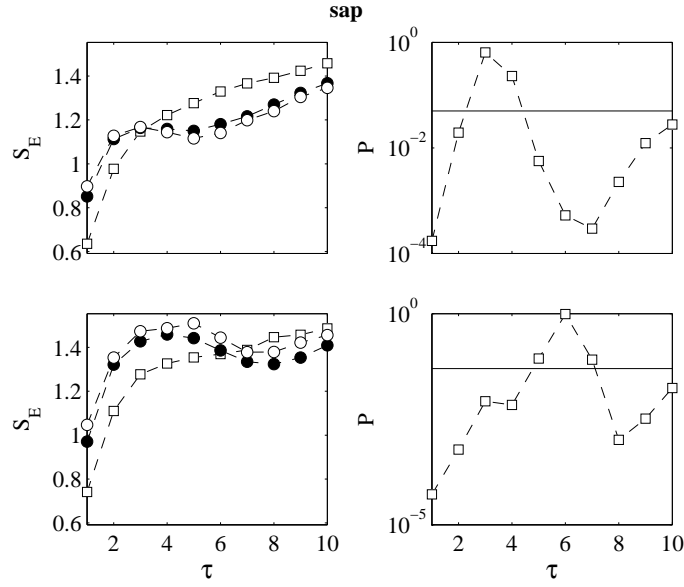


FIG. 3: Sample entropy of *sap* time series plotted versus τ . Empty squares are the averages over the 47 healthy subjects, full circles are the averages over the 275 CHF patients, and empty circles are the averages over the 54 patients for whom cardiac death occurred. Top left: S_E in basal condition. Top right: the probability that basal S_E values from controls and patients were drawn from the same distribution, evaluated by non parametric test. Bottom left: S_E in paced breathing condition. Bottom right: the probability that paced breathing S_E values from controls and patients were drawn from the same distribution, evaluated by non parametric test.

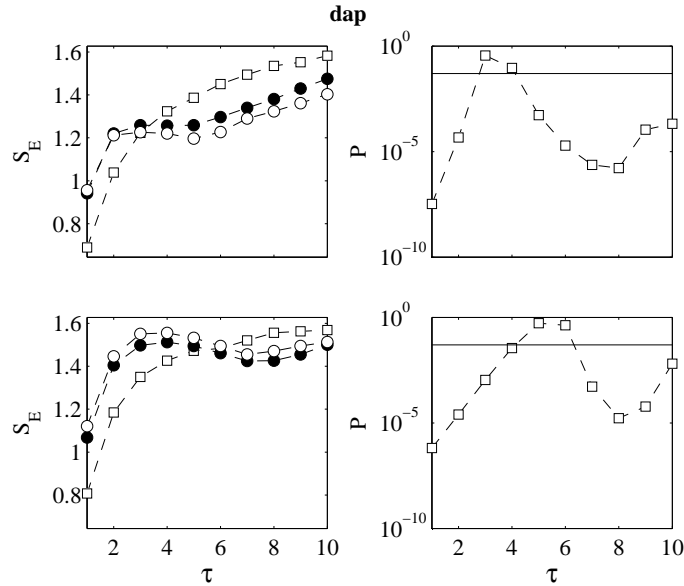


FIG. 4: Sample entropy of *dap* time series plotted versus τ . Empty squares are the averages over the 47 healthy subjects, full circles are the averages over the 275 CHF patients, and empty circles are the averages over the 54 patients for whom cardiac death occurred. Top left: S_E in basal condition. Top right: the probability that basal S_E values from controls and patients were drawn from the same distribution, evaluated by non parametric test. Bottom left: S_E in paced breathing condition. Bottom right: the probability that paced breathing S_E values from controls and patients were drawn from the same distribution, evaluated by non parametric test.

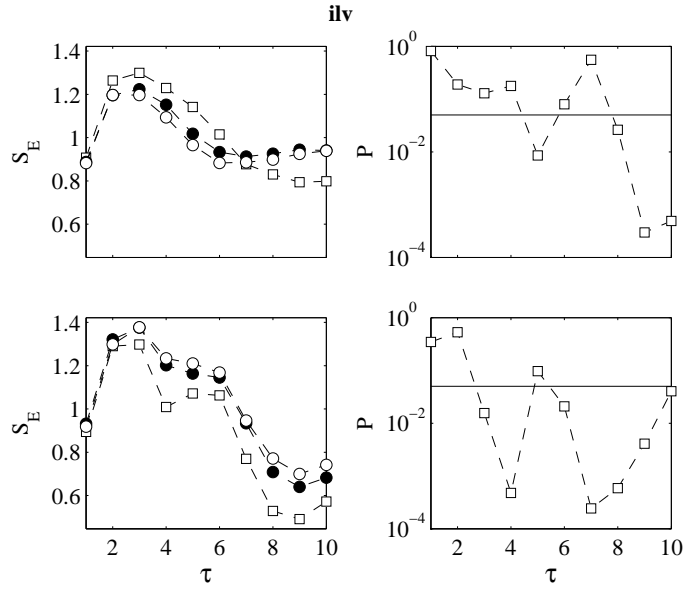


FIG. 5: Sample entropy of *ilv* time series plotted versus τ . Empty squares are the averages over the 47 healthy subjects, full circles are the averages over the 275 CHF patients, and empty circles are the averages over the 54 patients for whom cardiac death occurred. Top left: S_E in basal condition. Top right: the probability that basal S_E values from controls and patients were drawn from the same distribution, evaluated by non parametric test. Bottom left: S_E in paced breathing condition. Bottom right: the probability that paced breathing S_E values from controls and patients were drawn from the same distribution, evaluated by non parametric test.

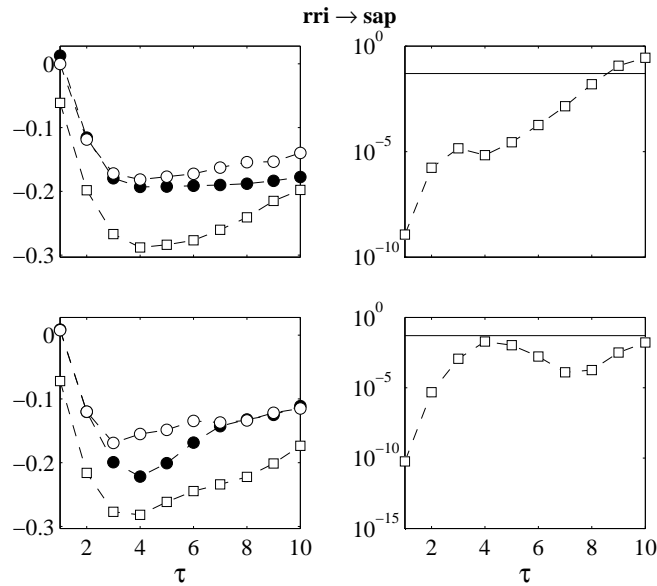


FIG. 6: The strength of the interaction *rri* \rightarrow *sap*, evaluated as described in the text, is plotted versus τ . Empty squares are the averages over controls, full circles are the averages over patients, and empty circles are the averages over dead patients. Top left: *rri* \rightarrow *sap* in basal condition. Top right: the probability that basal values from controls and patients were drawn from the same distribution, evaluated by non parametric test. Bottom left: *rri* \rightarrow *sap* in paced breathing condition. Bottom right: the probability that paced breathing values from controls and patients were drawn from the same distribution, evaluated by non parametric test.

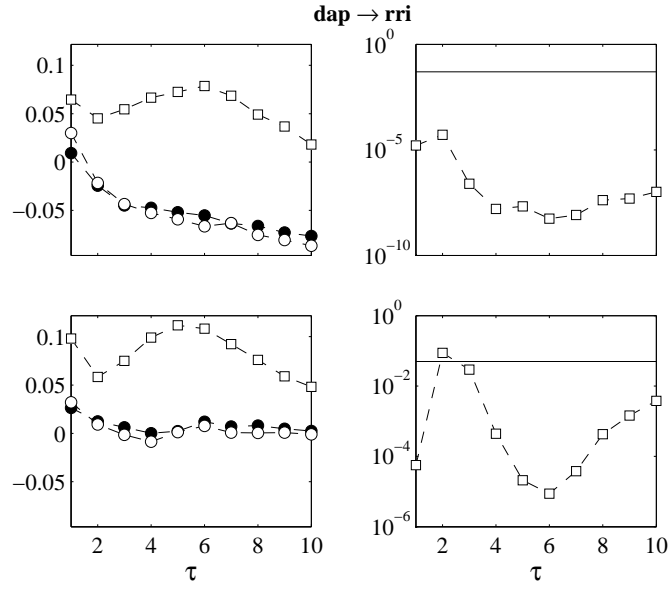


FIG. 7: The strength of the interaction $dap \rightarrow rri$, evaluated as described in the text, is plotted versus τ . Empty squares are the averages over controls, full circles are the averages over patients, and empty circles are the averages over dead patients. Top left: $dap \rightarrow rri$ in basal condition. Top right: the probability that basal values from controls and patients were drawn from the same distribution, evaluated by non parametric test. Bottom left: $dap \rightarrow rri$ in paced breathing condition. Bottom right: the probability that paced breathing values from controls and patients were drawn from the same distribution, evaluated by non parametric test.

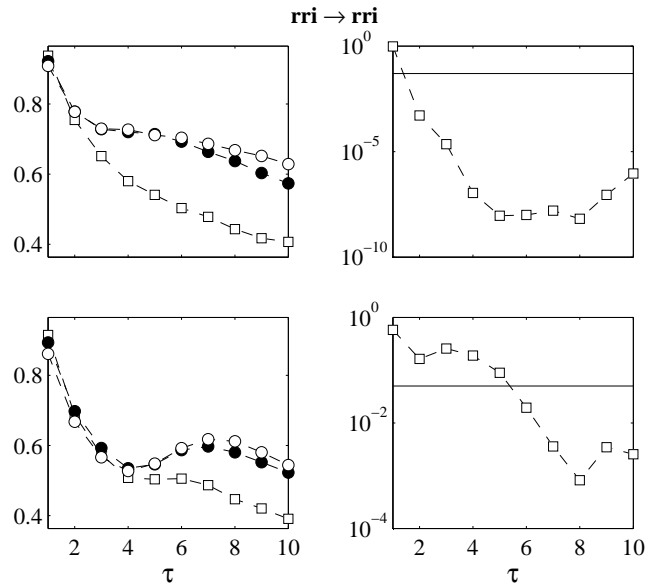


FIG. 8: The strength of the interaction $rri \rightarrow rri$, evaluated as described in the text, is plotted versus τ . Empty squares are the averages over controls, full circles are the averages over patients, and empty circles are the averages over dead patients. Top left: $rri \rightarrow rri$ in basal condition. Top right: the probability that basal values from controls and patients were drawn from the same distribution, evaluated by non parametric test. Bottom left: $rri \rightarrow rri$ in paced breathing condition. Bottom right: the probability that paced breathing values from controls and patients were drawn from the same distribution, evaluated by non parametric test.

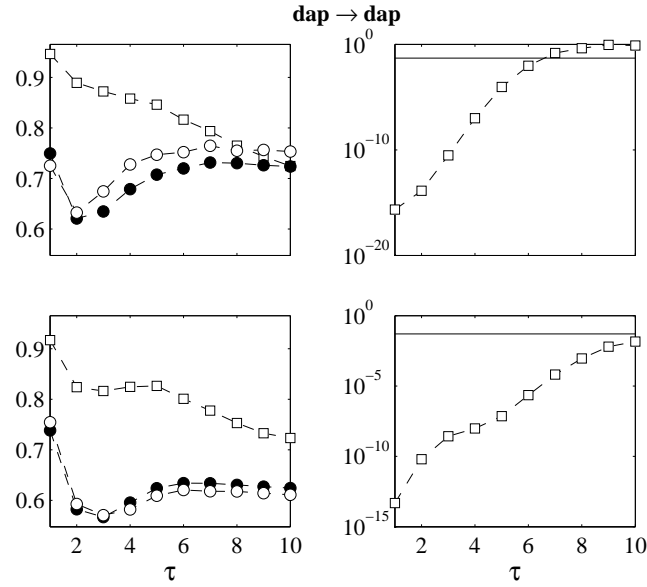


FIG. 9: The strength of the interaction $dap \rightarrow dap$, evaluated as described in the text, is plotted versus τ . Empty squares are the averages over controls, full circles are the averages over patients, and empty circles are the averages over dead patients. Top left: $dap \rightarrow dap$ in basal condition. Top right: the probability that basal values from controls and patients were drawn from the same distribution, evaluated by non parametric test. Bottom left: $dap \rightarrow dap$ in paced breathing condition. Bottom right: the probability that paced breathing values from controls and patients were drawn from the same distribution, evaluated by non parametric test.

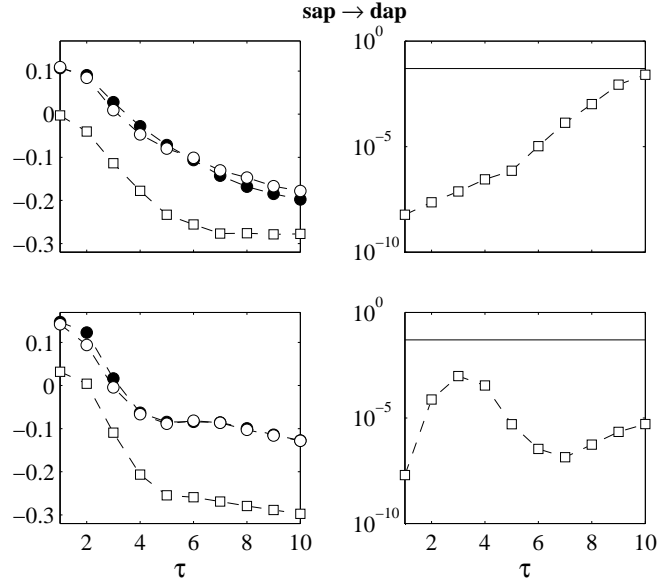


FIG. 10: The strength of the interaction $sap \rightarrow dap$, evaluated as described in the text, is plotted versus τ . Empty squares are the averages over controls, full circles are the averages over patients, and empty circles are the averages over dead patients. Top left: $sap \rightarrow dap$ in basal condition. Top right: the probability that basal values from controls and patients were drawn from the same distribution, evaluated by non parametric test. Bottom left: $sap \rightarrow dap$ in paced breathing condition. Bottom right: the probability that paced breathing values from controls and patients were drawn from the same distribution, evaluated by non parametric test.